A Space Phasor Based Current Hysteresis Controller Using Adjacent Inverter Voltage Vectors with Smooth Transition to Six Step Operation for a Three Phase Voltage Source Inverter

M. R. Baiju, K. K. Mohapatra, R. S. Kanchan, P. N. Tekwani and K. Gopakumar, CEDT, Indian Institute of Science, Bangalore, India

Keywords: Current controlled inverter, Space phasor based hysteresis controller

Abstract

In this paper, a space phasor based current hysteresis controller for a three-phase voltage source inverter is proposed. The current errors are determined along three axes, which are orthogonal to the A, B, C phases, and the current error space phasor is held within a hexagonal boundary. The proposed controller does not require any computation of machine voltage vector and uses only those inverter voltage vectors, which are adjacent to the machine voltage vector for the entire range of operation. The region detection logic employed in the proposed controller ensures that, the vector (among the three adjacent vectors), which has the largest deviation in the opposite direction, is selected, for all the regions of the hexagonal boundary. A simple self-adapting logic is used to effect sector changes and smooth transition to six-step mode of operation is achieved. The proposed controller is implemented for a 5hp induction motor drive.

Introduction

Performance of a drive system mainly depends on the quality of the current loop and therefore, efficient current control of PWM inverters is very important in high dynamic performance applications. The current controlled PWM inverters are well suited for high performance drive applications. In the current controlled inverters, the hysteresis controllers are extensively used due to their inherent simplicity and fast dynamic response [1-2]. The hysteresis controllers can be broadly classified into two categories. (a) conventional hysteresis controllers (b) space phasor based hysteresis controllers. In the conventional hysteresis controller, three independent hysteresis controllers are used for the three phases and the state of each leg of the inverter is independently determined by the hysteresis controller, in the respective phase. These controllers result in high frequency switching due to limit cycle operation and have sub-harmonic oscillations [3-5]. Also, independent hysteresis controller for the three phases, results in wide switching frequency variation, depending on the load parameter variation and with output AC voltage. The variations in the switching frequency can be controlled, by changing the tolerance band according to the output AC voltage amplitude [6-8]. These types of schemes are very complex to implement and the simplicity of the conventional hysteresis controller is also lost. The switching frequency variations, with output voltage, for a conventional independent controller is presented in [9]. The space phasor based hysteresis controllers operate on the current error space phasor, which reflects the combined effect of the current errors on the A, B, C phases of the induction motor. The current error space phasor is kept within a boundary by choosing an inverter voltage vector which will bring back the error space phasor whenever the error space phasor goes beyond this boundary [10-17]. The space phasor based hysteresis controllers utilize the zero vector also along with the non zero vectors and this results in reducing the switching frequency [10]. Though it needs extensive off line computation and complex implementation schemes, predictive controllers proposed in reference [11] achieves optimum PWM switching and minimum switching frequency. The hysteresis regulator presented in reference [12] achieves fast response during transients by choosing vectors with largest current error deviation in the opposite direction whenever current error becomes very large during transients. But this results in non-optimum PWM switching and also this scheme needs estimation of back emf from the high frequency current error derivatives. In reference [13], a space phasor based hysteresis controllers is presented where the current error is represented in the orthogonal d-q axes and appropriate vectors are selected to keep the current error within a rectangular boundary. This controller has good dynamic response and use simple look up tables to select the inverter vectors. However it does not always ensure optimum PWM switching, as the nearest vectors to the machine voltage vector is not always selected. In reference [14] and [15] space phasor based hysteresis controller with adaptive switching pattern schemes are proposed to achieve reduced inverter switching. But these schemes do not explain the operation in over modulation region extending to six-step mode. Multi axis hysteresis controllers monitor current errors along three 120° axes resulting in a hexagonal boundary [16, 17]. In the multi axis space phasor based hysteresis regulator presented in [17], the current error space phasor is represented on three axes which are perpendicular to the A, B, C axes. This multi axis space phasor based controller always chooses one of the nearest vectors to limit the current error space phasor within a hexagonal boundary. This ensures optimum PWM switching and does not need any information of the back emf vector. In this scheme, the hexagonal boundary region for inverter vector selection forming a triangular sector is not properly selected and hence results in high frequency PWM switching at the hexagonal corners. Also, the over modulation region boundaries are not properly selected.

In this paper, a multi axis current hysteresis controller, where the current error space phasor is kept within a hexagonal boundary, is presented. A suitable inverter voltage vector is selected whenever the current error space phasor hits the hexagonal boundary, using

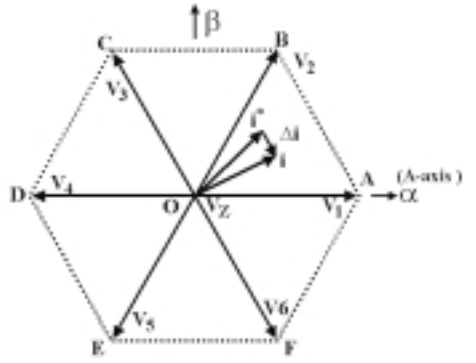

Fig.1: The inverter voltage vectors and the current error space phasor

a simple look up table. The regions in the hexagonal boundary are determined such that, whenever the current error hits the boundary, the voltage vector (among the three adjacent vectors) which will result in the largest current error deviation away from the boundary is selected. The proposed scheme also eliminates the high frequency hexagonal corner boundary switching, by properly identifying the boundary regions for the inverter vector selection. Simple look up tables are used for the PWM generation and the proposed scheme works well in the over modulation region, with a smooth transition to the six-step mode operation.

Principle of the space vector based hysteresis controllers

The space vector based hysteresis controllers use the concept of the current error space phasor, which represents the combined effect of the current errors in the individual phases. Fig. 1 shows the inverter voltage vectors, six active vectors ($\mathbf{V_1}$ to $\mathbf{V_6}$) and the zero voltage vector $\mathbf{V_Z}$, with vector $\mathbf{V_1}$ oriented along the A-phase axis. While the voltage vectors from the inverter can only take these discreet vectors along with the zero voltage vector, the reference current space vector and the actual machine current space vector can have any position.

In Fig. 1, ***i*** and ***i**** show the actual machine current space vector and the reference current space phasor respectively at a particular instant. The current error space phasor or the current deviation vector; $\Delta\mathbf{i}$, can be defined as [10, 13, 17].

$$\Delta \boldsymbol{i} = \boldsymbol{i} - \boldsymbol{i}^* \tag{1}$$

The current deviation vector is the resultant of the individual current errors in the three phases. If Δi_a, Δi_b and Δi_c are the instantaneous current errors along the A, B, C phases respectively, the current error space phasor can be viewed as the vector sum of these individual current errors as shown by (2),

$$\Delta \mathrm{i} = \Delta i_a + \Delta i_b \, e^{j2\pi/3} + \Delta i_b \, e^{j4\pi/3} \tag{2}$$

The basic principle of the space vector based controllers is to select an appropriate inverter voltage vector so that current error space phasor is kept within an appropriate boundary. The relation between the inverter voltage vector $\mathbf{v}[k]$ and the current error space phasor can be derived as following:

The voltage equation for a three-phase voltage source inverter is given by (3), where $\boldsymbol{V}_b$ is the back emf vector, $\boldsymbol{L}_\sigma$ is the stator leakage inductance and R_s is the stator resistance.

$$\mathbf{v}[k] = L_s \frac{di}{dt} + R_s i + V_b \tag{3}$$

Substituting (1) in (3),

$$\mathbf{v}[k] - L_\sigma \frac{di^*}{dt} + Ri^* + L_\sigma \frac{d\Delta i}{dt} + R\Delta i + V_b \tag{4}$$

$$L_s \frac{d\Delta i}{dt} = (L_s \frac{di^*}{dt} + R_s i^* + V_b) + R_s \Delta i - \mathbf{v}[k] \tag{5}$$

Neglecting $R_s \, \Delta_\mathbf{i}$ (5) becomes,

$$L_s \frac{d\Delta i}{dt} = (L_s \frac{di^*}{dt} + R_s i^* + V_b) - \mathbf{v}[k] \tag{6}$$

In (6), the term $(L_\sigma \frac{di^*}{dt} + R_s i^* + V_b)$ can be expressed as $\boldsymbol{V}_m$, the machine voltage vector when the machine current is assumed to be equal to the reference current [6].

$$L_\sigma \frac{d\Delta i}{dt} = V_m - \mathbf{v}[k] \tag{7}$$

If the inverter voltage vector, $v[k]$ could be equal to $\boldsymbol{V}_m$ at every instant, the machine current would have been the same as the reference current, without any deviation. But since the inverter can generate only one of the eight distinct vectors, it would result in a current error deviation. From (7), the direction at which the current error space phasor moves is given by;

$$\frac{d\Delta i}{dt} = (V_m - \mathbf{v}[k]) \Big/ L_\sigma \tag{8}$$

Equation (8) shows that for a given $\boldsymbol{V}_m$, the current error space phasor moves in different directions for different inverter voltage vectors. When one inverter voltage vector is applied, the current error moves in a particular direction and hits the hysteresis boundary in that direction. The space phasor based hysteresis controller then applies another inverter voltage vector, which would result in the error vector moving in the opposite direction (i.e. away from the boundary) so that error space phasor is brought back into the boundary.

This means that the switchings in the individual phases are coordinated to get the desired inverter voltage at every instant. Different strategies have been proposed to choose the desired inverter voltage vector to keep the current error space phasor within the boundary [10-17]. The boundary for the current error depends on the axis along which the individual current errors are monitored. If the current error space phasor is seen as the sum of two orthogonal currents, the current error space phasor is limited within a rectangular boundary [10, 13]. If the current errors are monitored along a set of three 120 degree separated axes, it results in the current error space phasor being kept within a hexagonal boundary [12, 16, 17].

In reference [17], a space phasor based hysteresis controller is presented where the current errors are monitored along three axes j_A, j_B, j_C which are mutually perpendicular to the A, B, C axes. The current error space phasor is kept within a hexagonal boundary by applying an inverter voltage vector among the three adjacent vectors, which will bring down the error whenever the hexagonal boundary is hit. It does not use any computation to determine the position of the back emf vector and when the current error space phasor hits a region of the hexagonal boundary, an inverter voltage vector among the nearest three vectors to the machine back emf vector is selected. A region detector is used to identify the region of the hexagonal boundary hit by the current error space phasor. But the region decoder employed in reference [17] does not ensure that the voltage vector with largest error deviation is selected for all the regions of the hexagonal boundary. In the present work, a modified region detector is used so that every region in the hexagonal boundary is uniquely associated with an inverter voltage vector which has the largest error deviation in the opposite direction so that the error space phasor is brought within the hexagonal boundary, quickly. Also, the high frequency inverter switching at the hexagonal corner boundary is avoided in the scheme.

The proposed space phasor based current hysteresis controller

In the proposed space phasor based hysteresis controller, the current error space phasor is kept within a boundary, by applying one of the three inverter voltage vectors which are adjacent to the machine voltage vector $\boldsymbol{V}_m$. This feature of adjacent vector selection is retained for the entire speed range of operation. Fig. 2 shows the inverter voltage vectors and the machine voltage vector $\boldsymbol{V}_m$ for two positions of machine voltage vector. When the machine voltage vector $\boldsymbol{V}_m$ is in sector-1, let us consider the directions of the current error space phasor when the three adjacent vectors $\mathbf{V_1}$, $\mathbf{V_2}$ and $\mathbf{V_Z}$ are switched.

In Fig.2, when $\mathbf{V_1}$ is switched, the current error space phasor will move in the direction **PA** and when $\mathbf{V_2}$ is switched, the error space phasor will move in the direction of **PB** (equation (8)). When the zero voltage vector $\mathbf{V_Z}$ is switched, the error space phasor will move in the direction of **OP'**. It may be noted that these directions correspond to the particular instant when the machine voltage vector is located as **OP** and these directions will change with the position and amplitude of the machine voltage vector. But these directions for a particular inverter voltage vector ($\mathbf{V_1}$, $\mathbf{V_2}$, $\mathbf{V_Z}$ for sector-1) are confined within two directions each corresponding to the respective two boundaries of sector-1[11] . For example, when inverter voltage vector $\mathbf{V_1}$ is switched and when the machine voltage vector is along **OA** (which is the boundary between sector-1 and sector-6,) the error space phasor moves along **OA**. Similarly, for inverter voltage vector $\mathbf{V_1}$, the error space phasor will move in the direction of **OF** when the machine voltage vector is along **OB** (which is the boundary of sector-1 with sector-2). So, for any position of machine voltage vector within sector-1, when vector $\mathbf{V_1}$ is switched, the directions in which the error space phasor can move are confined within these two directions. In the same way, for sector-1, when $\mathbf{V_2}$ is switched the current error space phasor can move in any direction, confined within the directions of **OC** and **OB**. When zero voltage vector is switched the error space phasor directions are confined within the directions of **OD** and **OE** [17]. These three set of directions are shown in Fig.3. This set of directions can be used to define a boundary for the error space phasor, beyond which it should not be allowed to move. For example if the error space phasor moves in a direction parallel to any direction bounded by the directions of **OA** and **OF**, it can touch a boundary XZ as shown in Fig. 3.This boundary can be decided to be anywhere at a distance 'h' along the j_C axis.

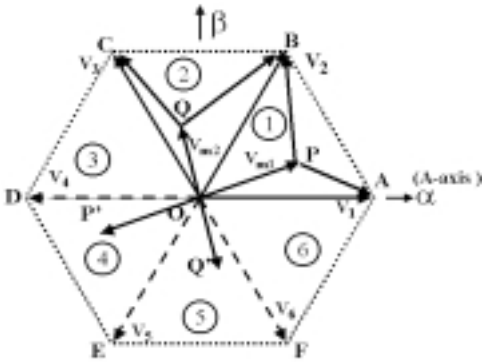

Fig. 2: The machine voltage vector and directions of current error space phasor

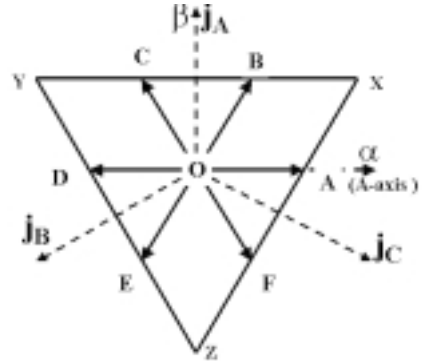

Fig. 3: The boundary of current error space phasor in Sector-1

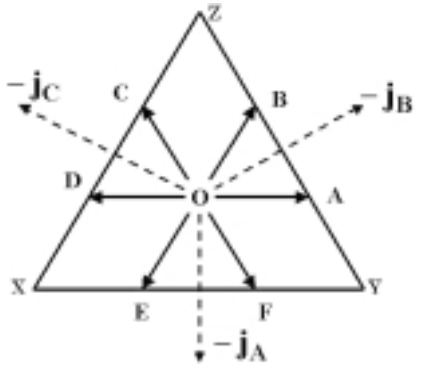

Fig. 4: The boundary of current error space phasor in Sector-2

Similarly, the directions **OC** and **OB** define another boundary YX along the j_A axis and the directions **OD** and **OE** define the third boundary along the j_B axis. Therefore, when the machine voltage vector is in sector-1, whenever $\mathbf{V_1}$ is switched, the current error space phasor will approach and hit the boundary XZ, in a particular direction which depends on the instantaneous position of the machine voltage vector (8). Similarly the error space phasor will hit the YX boundary when $\mathbf{V_2}$ is switched and will touch the YZ boundary when the zero voltage vector is switched. These three boundaries define a triangular boundary XYZ as in Fig. 3, the sides of the triangle being at a distance 'h' along the j_A, j_B and j_C axes. It can be verified that this same triangular boundary exists for all the odd sectors, i.e. sector 1, 3 and 5 [17].

When the machine voltage vector is in sector-2, the adjacent inverter voltage vectors to be switched are, $\mathbf{V_2}$, $\mathbf{V_3}$ and $\mathbf{V_Z}$.(Fig.1). In this case also we can determine the directions within which the error space phasor can move when each of these vectors are

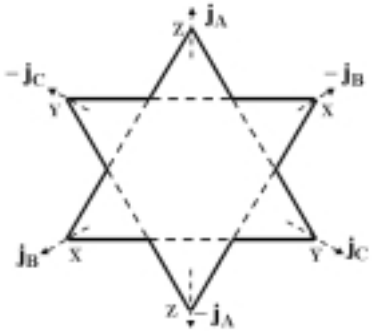

Fig. 5: The boundary of current error space phasor

switched. When $\mathbf{V_2}$ is switched, the directions within which the error space phasor can move are OA and OB. Similarly, the directions OC and OD correspond to $\mathbf{V_3}$ and the directions OE and OF correspond to $\mathbf{V_Z}$. These three sets of directions also will define a triangular boundary as shown in Fig. 4, where the three boundaries are along the $-j_A$, $-j_B$ and $-j_C$ axes. It can be verified that for all the even sectors (sector 2, 4 and 6; Fig. 2), the current error space phasor directions are bounded by this triangular boundary.

Fig. 5 shows the boundary within which the error space phasor can move when the machine voltage vector moves through all the sectors.

Selection of inverter voltage vector within each sector

The proposed hysteresis controller uses only vectors which are adjacent to the machine voltage vector. As mentioned earlier, within a sector, when a particular inverter voltage is switched, it makes the error space phasor to move towards one of the boundaries (Fig. 3 for odd sectors and Fig. 4 for the even sectors). The inverter voltage vector is continued till the error space phasor reaches another boundary. Once the space phasor hits the boundary, the inverter voltage vector is changed so that error space phasor is brought back within the boundary, and moves towards the opposite side of the triangular boundary. The proposed controller divides the triangular boundary to three regions and each of these regions is associated with a suitable inverter voltage vector (depending on the sector) which will take the error space phasor towards the opposite side of the triangular boundary.

Fig. 6a shows the regions and vectors for the sector-1. The triangular boundary is divided into three regions R_1, R_2 and R_3 as shown in Fig. 6a. As shown in Fig. 6a, when the error space phasor hit anywhere in the region R_1, the zero voltage vector $\mathbf{V_Z}$ is selected so that the error space phasor moves towards the opposite side. Similarly vector $\mathbf{V_1}$ and $\mathbf{V_2}$ are selected when the error space phasor is hitting the boundary in the R_2 and R_3 regions respectively. Fig. 6b shows the regions and the respective vectors for all the odd sectors (which all have the common triangular boundary), which would take the error space phasor away from each region. Fig. 6c shows the regions $\bar{R}_1$, $\bar{R}_2$ and $\bar{R}_3$ and the associated vectors for sector-2, and Fig. 6d shows the regions and vectors for all the even sectors.

It is shown that, for odd sectors the boundaries are placed along the j_A, j_B, j_C axes and for even sectors the boundaries are placed along the $-j_A$, $-j_B$, $-j_C$ axes and this would result in the combined boundary as shown in Fig. 5. It may be noted that, for this triangular boundary, the error space phasor moves to double the

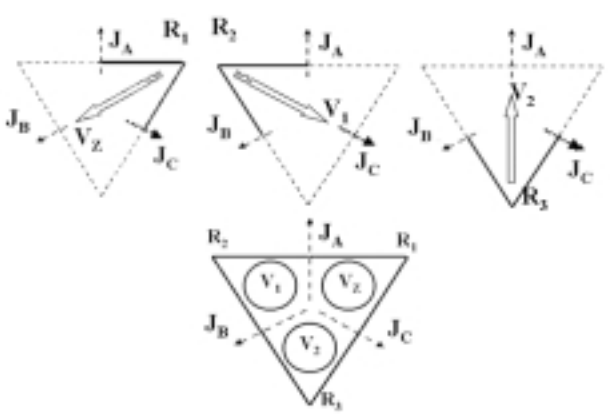

Fig. 6a: The regions and the vectors to be switched for sector-1

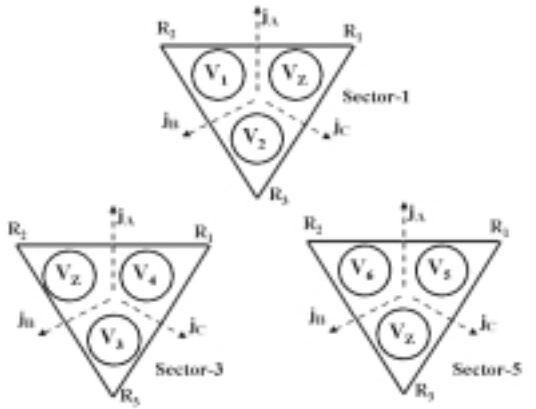

Fig. 6b: The regions and the vectors to be switched for the odd sectors

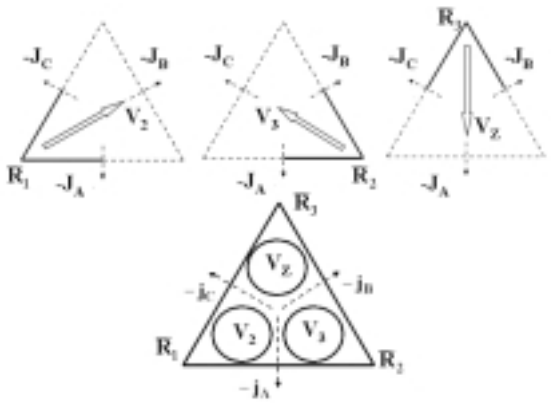

Fig. 6c: The regions and the vectors to be switched for sector-2

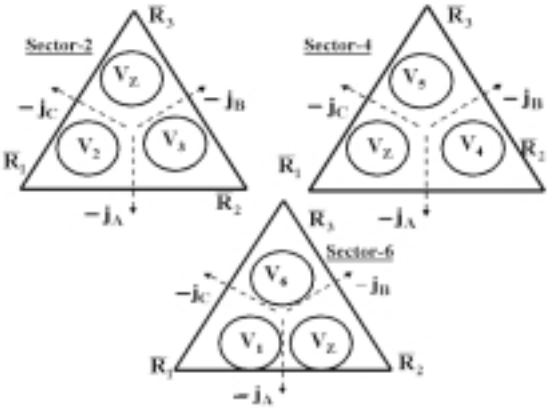

Fig. 6d: The regions and the vectors to be switched for even sectors

distance, along the $-j_A, -j_B, -j_C$ axes in the case of odd sectors and along j_A, j_B, j_C axes for the even sectors (Fig. 3 and Fig. 4). If we place boundaries along all these axes, for both odd as well as even sectors, we would get a hexagonal boundary as shown in Fig. 7.

In the proposed work, the hysteresis controller is implemented with this hexagonal boundary, where along all the six directions $(-j_A, -j_B, -j_C, j_A, j_B, j_C)$, the current error is held always within the hexagonal boundary limits. This hexagonal boundary can be divided into different regions consistent with regions of the triangular boundaries defined in Fig. 6a and Fig. 6c. Fig. 8a shows the different regions of the hexagonal boundary for the odd sectors ($\bar{R}_1$, $\bar{R}_2$, $\bar{R}_3$) and Fig. 8b shows the regions of the hexagonal boundary for the even sectors ($\bar{R}_1$, $\bar{R}_2$, $\bar{R}_3$).

Each region of the hexagonal boundary is associated with an unique vector for each sector as explained earlier (Fig. 6b and Fig. 6d), which will force the error space phasor to the opposite direction. The different regions and respective inverter voltage vectors to be switched are shown in Table 1.

Region detection and vector selection

The proposed hysteresis controller uses a hexagonal boundary which is divided into different regions R_1, R_2, R_3 for odd sectors and $\bar{R}_1$, $\bar{R}_2$, $\bar{R}_3$ for the even sectors. These regions can be identified using a simple logic based on the comparators placed along the j_A, j_B, j_C, $-j_A$, $-j_B$, and $-j_C$ axes. The current components along j_A, j_B, j_C axes can be computed for the A-phase and B-phase currents of the machine, using the following equations, where i_A, i_B and i_C are the actual machine phase currents [11].

$$i_{j_A} = \frac{\sqrt{3}}{2}\left(i_B - i_C\right) \quad i_{j_B} = \frac{\sqrt{3}}{2}\left(i_C - i_A\right) \quad i_{j_C} = -\left(i_{j_A} + i_{j_B}\right) \tag{9}$$

Then the current errors along these axes are

$$\Delta i_{j_A} = i_{j_A} - i^*_{j_A}, \quad \Delta i_{j_B} = i_{j_B} - i^*_{j_B}, \quad \Delta i_{j_A} = i_{j_C} - i^*_{j_C} \tag{10}$$

where i^*_{jA}, i^*_{jB}, i^*_{jC} are the components of the reference current along the j_A, j_B, j_C axes respectively.

Fig.9 shows the comparators along the axes.

The comparator remains OFF ('0') when the current error is within the hysteresis band in that direction. The comparator turns ON ('1') when the current error space phasor just crosses the hysteresis boundary through that particular side of the hexagonal boundary. Each side of the hexagonal boundary is divided into two segments as shown in the Fig.10 .The region detector logic identifies the segment through which the current error space phasor crosses the hexagonal boundary. This can be determined using a simple logic. For example, for sector-1, the current error space phasor hits the segment R_{a1}, if the j_A comparator is ON and the component of the current error along the j_B axis is greater than the current error component along the j_C axis, i.e. $\Delta i_{jB} \geq \Delta i_{jC}$. If $\Delta i_{jB} < \Delta i_{jC}$, it is clear that the error space phasor crosses through the segment R_{a2}. The logic to determine each of these segments is given below;

When $j_A = 1$; If $\Delta i_{jB} \geq \Delta i_{jC}$ segment is R_{a1}, else R_{a2}
When $j_B = 1$; If $\Delta i_{jC} \geq \Delta i_{jA}$ segment is R_{b1}, else R_{b2}
When $j_C = 1$; If $\Delta i_{jA} \geq \Delta i_{jB}$ segment is R_{c1}, else R_{c2}
When $-j_A = 1$; If $\Delta i_{jB} \geq \Delta i_{jC}$ segment is $\bar{R}_{a2}$, else $\bar{R}_{a1}$
When $-j_B = 1$; If $\Delta i_{jC} \geq \Delta i_{jA}$ segment is $\bar{R}_{b2}$, else $\bar{R}_{b1}$
When $-j_C = 1$; If $\Delta i_{jA} \geq \Delta i_{jB}$ segment is $\bar{R}_{c2}$, else $\bar{R}_{c1}$

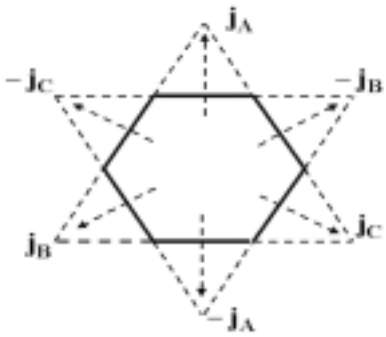

Fig. 7: The hexagonal boundary for the current error space phasor

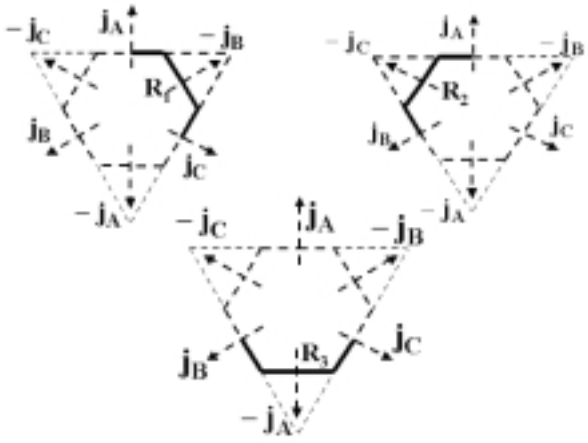

Fig. 8a: The regions and the vectors to be switched for odd sectors

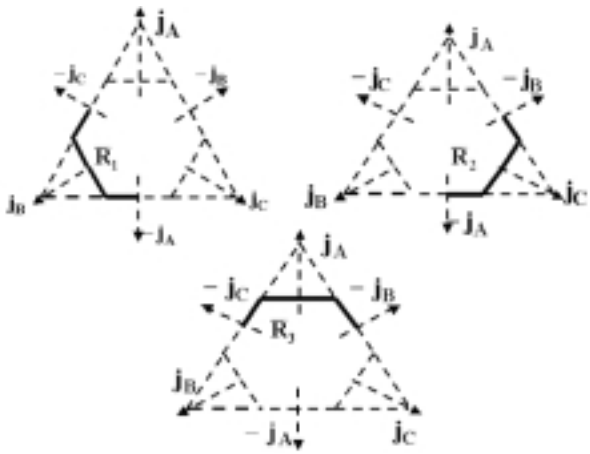

Fig. 8b: The regions and the vectors to be switched for even sectors

Table 1: The regions of the hexagonal boundary and the inverter voltage vectors

Sector	Regions					
	R_1	R_2	R_3	$\bar{R}_1$	$\bar{R}_2$	$\bar{R}_3$
1	V_Z	V_1	V_2	*	*	*
2	*	*	*	V_2	V_3	V_Z
3	V_3	V_Z	V_4	*	*	*
4	*	*	*	V_Z	V_4	V_5
5	V_5	V_6	V_Z	*	*	*
6	*	*	*	V_1	V_Z	V_6

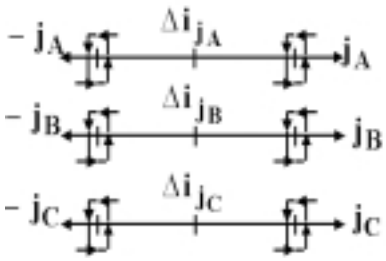

Fig. 9: The inner comparators (for vector selection)

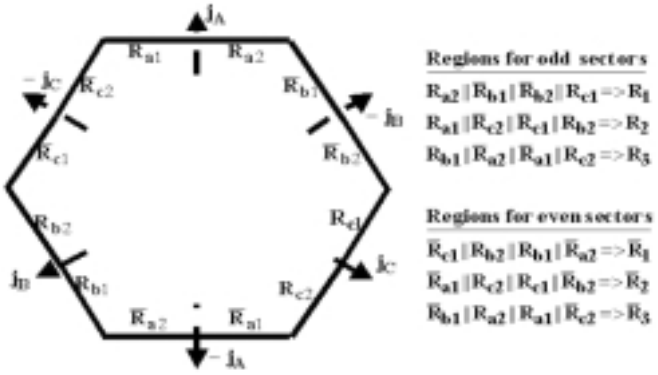

Fig. 10: The regions and the segments for the hexagonal boundary

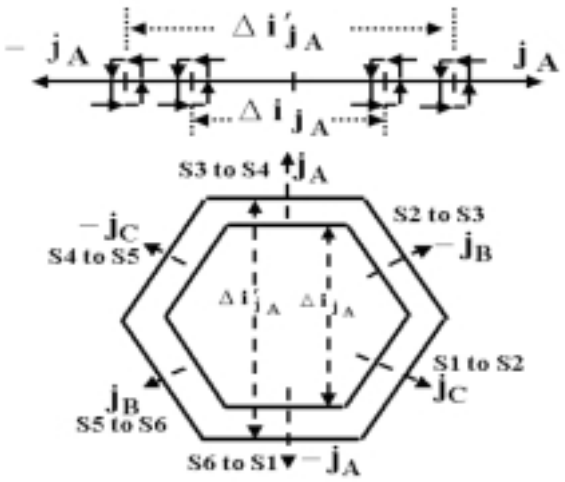

Fig.11: The outer hysteresis band and the directions of current error space phasor during sector change

It may be observed from Fig. 10 that each region of the hysteresis boundary (as defined in Fig. 8a and Fig. 8b) is composed of four segments. For example, the region R_1 is composed of the segments R_{a2}, $\bar{R}_{b1}$, $\bar{R}_{b2}$ and $\bar{R}_{c1}$. If the current error space phasor touches the hexagonal boundary along any one these four segments, the region is identified as R_1. Similarly, all the regions can be identified using similar relations as shown in Fig.10. Once the region is determined the inverter voltage vector to be switched to bring the current error back into the hysteresis boundary is selected using a look table (Table 1) as explained before.

High frequency switching between two vectors can occur, while the current error hits the hexagonal boundaries exactly along the axes. For example, let us assume that the current error crosses the hexagonal boundary exactly through the j_A axis. The j_A axis forms the boundary between region R_1 and R_2. Hence, the region detection logic while tracking the error space phasor will briefly switch between R_1 and R_2. The controller then will switch between $\mathbf{V_Z}$ and $\mathbf{V_1}$ and this would result in high frequency switching of the inverter. This would appear as a high frequency 'jitter' in the inverter output. In the proposed hysteresis controller such high frequency switching along the axes are avoided by a simple logic. When the current error crosses the hexagonal boundary along j_A axis, the j_A comparator will be 'ON' and it will remain ON, till the error is brought back within the hexagonal boundary, by vectors $\mathbf{V_Z}$ or $\mathbf{V_2}$. Since the j_A axis is exactly the boundary between R_1 and R_2, any of these vectors $\mathbf{V_1}$ and $\mathbf{V_Z}$, can bring back the error space phasor. Therefore, once a vector is selected, the proposed controller selects a new vector only if the current error space phasor comes within the hexagonal boundary and hits the boundary at some other region. Till then the previous vector is persisted. This technique will ensure that, once a vector is selected (which will definitely bring the error back to the boundary) the same vector is continued till the error space phasor hits the hexagonal boundary in another region. This will naturally avoid all high frequency switching that may occur between two vectors, when the current error hits the boundary exactly along the axes.

Self adaptive sector selection logic

The proposed hysteresis controller use s a self-adapting logic to identify the instants at which the machine voltage vector crosses from one sector to another. This sector change is identified with the help of another set of comparators placed a little further than the comparators used for the vector selection [17]. The comparators for the vector selection and sector selection along the j_A axis are shown in Fig. 11 Similar comparators are used in other axes also.

Let us consider the situation when the machine voltage vector moves from sector-1 to sector-2. It may be noted that when the machine voltage vector is very close to the boundary of sector 1 and sector-2, the vector selected would be either $\mathbf{V_2}$ or $\mathbf{V_Z}$ as these are near to machine voltage vector and hence would result in smaller deviation of the error space phasor (parallel to R_{c1} and R_{c2}, Fig. 10). When the machine voltage vector is along **OB** (Fig. 2), the current error would be moving in direction parallel to the **OB** direction when $\mathbf{V_2}$ is switched and it will be parallel to OF when $\mathbf{V_Z}$ is switched. In both the cases, the rate of change of current error along the j_C axis will be zero as these directions (OB and **OE**) are perpendicular to the j_C axis. Now, let us assume that, the machine voltage vector crosses to sector-2. As the machine voltage crosses over to sector-2, the deviation of current error space phasor will increase in the j_C direction and may cross the hexagonal boundary. The controller is yet to detect the sector change and the controller takes all action as if the machine voltage vector is in sector-1. Therefore, the region detection logic will identify that the current error space phasor has crossed the segment R_{c1} or R_{c2} and still the vector selected will be $\mathbf{V_2}$ or $\mathbf{V_Z}$. This will further increase the current error deviation in the j_C axis and the outer comparator along the j_C axis also will turn ON. This can be used to detect that the machine voltage vector has moved over to sector-2, and the sector changing logic updates the current sector as sector-2. Now the region detection logic will identify that the current error has hit the region R_2 (j_C axis for sector-2 and all even sectors, is included in region R_2, Fig. 8b) and vector $\mathbf{V_3}$ will be selected (Table-1), which will bring the current error within the hexagonal boundary. Therefore, the crossing over of $\mathbf{V_m}$ from sector-1 to sector-2 is uniquely identified, with the state of the outer comparator along j_C axis. It can be verified that, that if the machine vector moves from the sector-2 to sector-1 (i.e. the motor rotates in the opposite direction) the current error will increase through the $-j_C$ axis.

Therefore, whenever the machine voltage vector crosses from one sector to the next sector, the current error will increase along a

Table.2: The look-up table for sector selection [* means continue with the present sector]

Sector	The direction in which current error crosses the outer comparators					
	j_A	j_B	j_C	$-j_A$	$-j_B$	$-j_C$
1	6	*	2	*	*	*
2	*	*	*	*	3	1
3	4	2	*	*	*	*
4	*	*	*	3	*	5
5	*	6	4	*	*	*
6	*	*	*	1	5	*

Table 3: The look-up table for sector selection for the conditions two outer comparators are switched

Sector	The comparator pairs (regions where two comparators will be ON)					
	j_A $-j_B$	j_A $-j_C$	j_B $-j_C$	j_B $-j_A$	j_C $-j_A$	j_C $-j_B$
1	6	*	*	*	2	*
2	*	1	*	*	*	3
3	4	*	2	*	*	*
4	*	5	*	3	*	*
5	*	*	6	*	4	*
6	*	*	*	1	*	5

unique axis (which is the axis perpendicular to the boundary) and this is identified from the state of the outer comparators. The directions for sector change can be similarly identified also for the case where the machine voltage vector is rotating in the clockwise direction (reverse direction). Here the sector changes happen through the axis, which is opposite to that for the corresponding sector change in the forward direction [17]. For example, the sector change from sector-1 to sector-2 is through the j_C axis and the sector change from sector-2 to sector-1 (reverse speed operation) is through $-j_C$ axis. Fig. 11 shows the axes along which the current error would cross the outer hexagonal boundary, when the machine voltage rotates in the anti-clock wise direction. The look-up table for the sector selection (for both directions) is given Table 2.

Operation of the proposed controller during over modulation

When the motor is running in the higher speed regions, the machine voltage vector will be moving fast and will have a large amplitude since the motor back emf will be high (equation (6) and (7)). Fig. 13a shows the situation where the machine voltage vector $\mathbf{V_m}$ (**OP**), has a large amplitude and is outside sector-1. **PA** and **PB** are the directions in which the current error space phasor will move when vector $\mathbf{V_1}$ and $\mathbf{V_2}$ are switched respectively. Fig. 13a, also shows the trajectory of the current error space phasor, where the current error space phasor will be alternatively hitting the regions R_2 and R_3 while $\mathbf{V_1}$ and $\mathbf{V_2}$ are switched. If the current error space phasor hits the hysteresis band in the region R_3 at D as shown in Fig. 13a, the controller will switch vector $\mathbf{V_2}$ (Fig. 8a, Table 1).

Now the current error will move along **DE** which is parallel to the direction of **PB** (Fig. 13a) and will hit the boundary at E (region R_2) upon which vector $\mathbf{V_1}$ will be selected, taking the current error space phasor along **EF** (which is parallel to **PA**) and will again hit the hysteresis boundary in region R_3. This alternation between regions R_2 and R_3 (and vectors $\mathbf{V_1}$ and $\mathbf{V_2}$) will continue resulting in the current error space phasor coming out of the hysteresis boundary through the j_B axis as shown in Fig. 13a. The proposed controller detects this movement of the current error through the j_B axis when it crosses the outer hysteresis band and it changes the sector from sector-1 to sector-2.

Fig. 13b shows the current error space phasor with new regions for sector-2, and it can be observed that present position of the current error space phasor falls in the region $\bar{R}_1$ of sector-2. Previously, the current error space phasor could have crossed the outer hysteresis band with $\mathbf{V_1}$ or $\mathbf{V_2}$ depending on the outer hysteresis band and the speed at which the machine voltage vector is moving. But once the controller has updated the sector as sector-2, the controller will output $\mathbf{V_2}$, as the current error space phasor is in the region $\bar{R}_1$ (Fig. 8b, Table-1). Hence the current error space phasor will continue to move away from the hysteresis boundary with vector $\mathbf{V_2}$ as shown in Fig. 13b. It may be noted that the controller has advanced to sector-2, but the machine voltage vector may still be from sector-1 (but it should be that $\mathbf{V_2}$ is an inverter vector used in sector-1 and sector-2). Since the machine voltage vector is

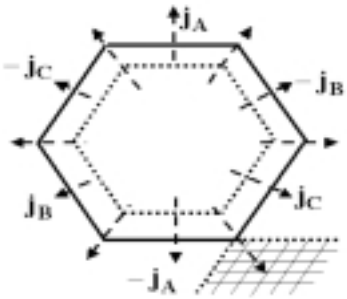

Fig. 12: The regions where two outer comparators will be switched during sector change

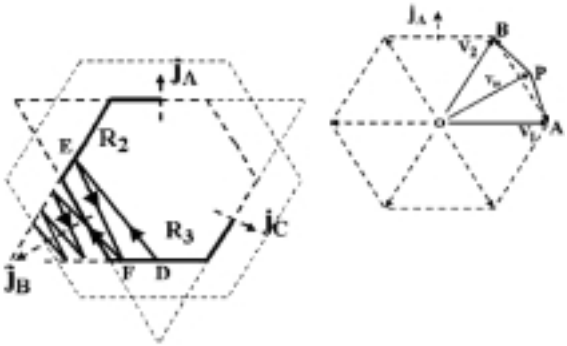

Fig. 13a: the current error space phasor trajectory during over modulation when the machine voltage in sector-1

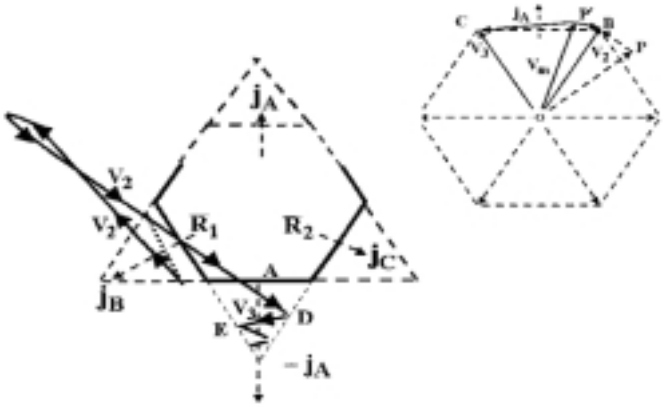

Fig. 13b: the current error space phasor trajectory during over modulation when the machine voltage in sector-2

Table 4: The sector selection logic including over modulation

Sector	The direction in which current error crosses the outer comparators					
	j_A	j_B	j_C	$-j_A$	$-j_B$	$-j_C$
1	6	2/6	2	*	*	*
2	*	*	*	3/1	3	1
3	4	2	4/2	*	*	*
4	*	*	*	3	5/3	5
5	6/4	6	4	*	*	*
6	*	*	*	1	5	1/6

moving very fast it will soon cross to sector-2 (still the inverter voltage vector is $\mathbf{V_2}$). Fig. 13b also shows the directions of the current error space phasor situation where the machine voltage vector is moving from sector-1 to sector-2 during over modulation. P'B and P'C are the directions movement of the current error space phasor in sector-2 for vectors $\mathbf{V_2}$ and $\mathbf{V_3}$ respectively. As the current error space phasor continues to move away from the hysteresis boundary (with vector $\mathbf{V_2}$), the machine voltage vector crosses over to sector-2 and now this forces the current error to reverse its course (since it has to move now in a direction parallel to **P'B** since the inverter vector is still $\mathbf{V_2}$).

The current error space phasor thus reverses and moves back towards the hysteresis boundary and hits the $\bar{R}_2$ region at D as shown in Fig. 13b upon which the controller selects vector $\mathbf{V_3}$. When vector $\mathbf{V_3}$ is switched, the current space phasor moves along **DE** (which is in the same direction as P'C) and alternate switchings between $\mathbf{V_3}$ and $\mathbf{V_2}$ will take the current error space phasor out through the $-j_A$ axis (Fig. 13b) and then the sector is advanced from sector-2 to sector-3. The current error space phasor moves through similar paths as the machine voltage vector moves from sector to sector during over modulation. For every sector there is a unique axis along which the current error will move out of the hexagonal boundary during over modulation, and the controller detects this with the state of the outer comparators and effects the sector change. Finally, the controller smoothly transits into the six-step mode of operation, where only one vector will be selected for every 60 degree.

The directions through which the current error space phase phasor will move out for the reverse direction during over modulation, can also be determined in a similar manner. In the forward direction during over modulation, the sector change from sector-2 to sector-3 is made when the current error space phasor moves out of the outer hysteresis band through the $-j_A$ axis. This is because, before the sector change from sector-2 to sector-1, the alternate switching between vectors $\mathbf{V_2}$ and $\mathbf{V_3}$ will take the error through the $-j_A$ axis (Fig. 13b). When the motor is rotating in the opposite direction (i.e. machine voltage vector is rotating in the clock wise direction), before the sector changes from sector-2 to sector-1, during over modulation vectors $\mathbf{V_2}$ and $\mathbf{V_3}$ will be switching alternatively and this takes the error space phasor through the $-j_A$ axis (as in Fig. 13b), and when the current error space phasor crosses the hysteresis boundary the sector is changed from sector-2 to sector-1. It may be noted that, during over modulation, the sector change from sector-2 to sector-3 (forward direction) as well as the sector change from sector-2 to sector-1 (reverse direction) are made when the current error moves out through the same axis ($-j_A$). The proposed controller therefore uses the direction information from the drive controller to make the appropriate sector change during over modulation. Table 4 gives the logic for sector change including the over modulation region.

Selection of the zero vector

In any sector the zero voltage vector can be realised two inverter states '+ + +' or by '– – –'. In the proposed controller, the zero vector is selected depending upon the previous vector. If the previous vector was either $\mathbf{V_1}$ ('+ – –'), $\mathbf{V_3}$ ('– + –') or $\mathbf{V_5}$ ('– – +') the zero vector is chosen as '– – –' so that transition to the zero vector is achieved, with switching of one inverter leg only [11]. If the previous vector was either $\mathbf{V_2}$ ('++ –'), $\mathbf{V_4}$ ('– ++') or $\mathbf{V_6}$ ('+ – +') the zero vector is realised by '+ + +'. Similarly, the transition from the zero vector to the active vector is also modified so that only inverter leg is switched [8]. If the previous zero vector is '+ + +', the next active vector is chosen as '++ –' or '– + +' or '+ – +', depending upon the sector. If the previous zero vector is '– – –', the next active vector is chosen as '+ – –' or '– + –' or '– – +'. This will avoid double switchings during transition from zero vector to the active vector. The insertion of a transition state will only result in a small instantaneous deviation in current error, which is negligible [8]. In this way, the proposed controller output optimum inverter vector states for the entire modulation range, with simple look-up table logic.

Simulation results

Fig.14 shows the simulation results for the proposed hysteresis controller. The hexagonal boundary the current error space phasor is shown in Fig. 14.a. The current error space phasor is held within the hexagonal boundary (Δi_{jA} = 0.6 Amp; Fig. 11). The instances seen in the figure where the current error briefly comes out of the hexagonal boundary corresponds to the sector change

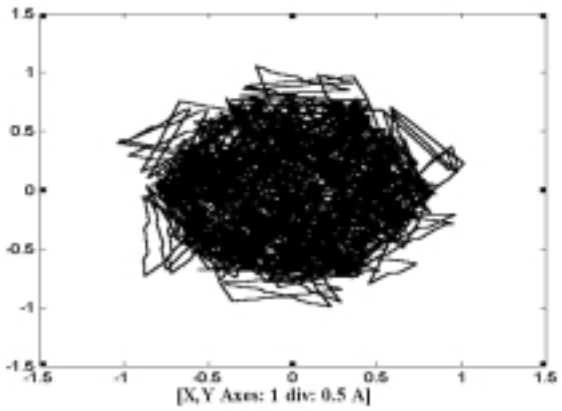

Fig. 14a: The current error space phasor boundary

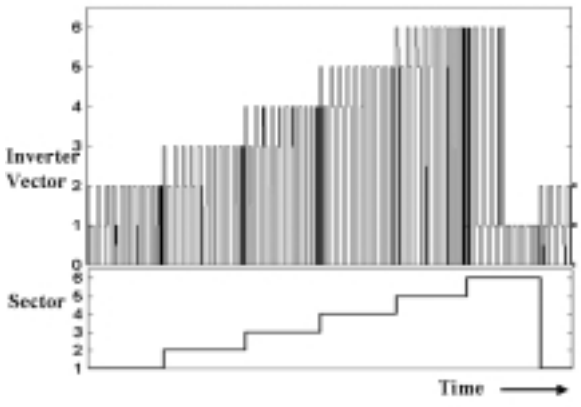

Fig. 14b: The sectors and the inverter vectors selected by the proposed controller

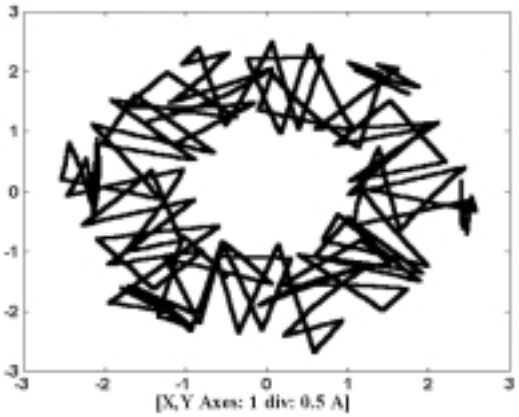

Fig. 14c: The machine current space phasor

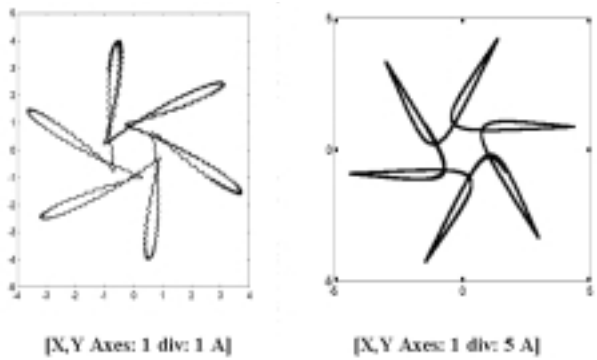

Fig. 14d: The current error space boundary (Left) and the current space phasor (Right) during six-step operation

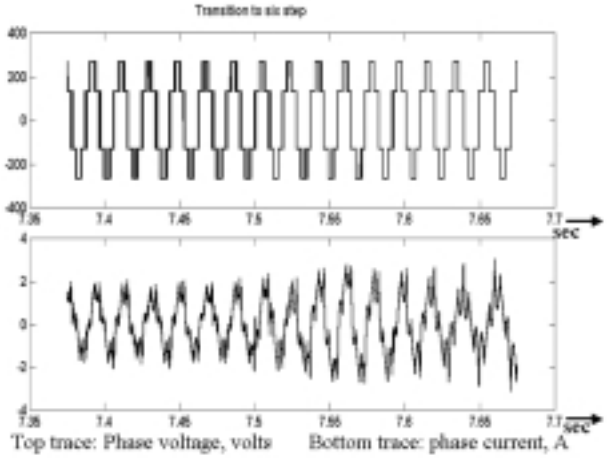

Fig. 14e: Transition to six-step mode operation, Top trace:Yaxis-200Volts/div, BottomTrace:Y-axis-2Amp/div

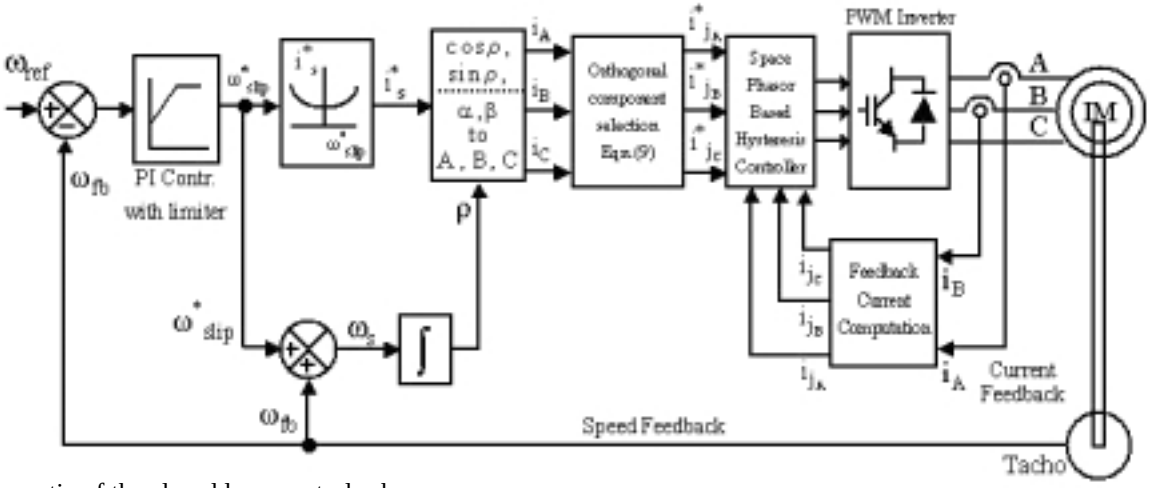

Fig. 15: Schematic of the closed loop control scheme

($\Delta i'_{jA}$ = 1 Amp; Fig. 11). Fig. 14b shows the vectors selected in different sectors and it is seen that only adjacent vectors are selected in all the sectors. Fig. 14c shows the machine current space vector. Fig. 14d shows the error space phasor boundary and the current space vector during the six-step operation. During six-step operation, the current error becomes large and hence always remains outside the outer hexagonal boundary. The transition to six-step is seen in Fig.14e and the proposed controller gives a smooth transition to six-step operation.

Experimental results

The proposed hysteresis controller is implemented for a 5hp induction motor drive with v/f control. The complete controller including the comparators is implemented on the TMSF2407 DSP platform. The three phase reference currents are generated depending on the frequency command and the controller is tested with drive for the entire speed range. The overall control structure and system interface with induction motor are as shown in Fig. 15.

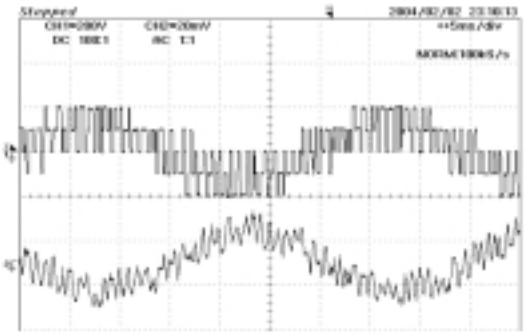

Fig.16a: The machine phase voltage and current
[Y axis: 1 div = 200 V Y-axis -: 1 div = 2 Amp]

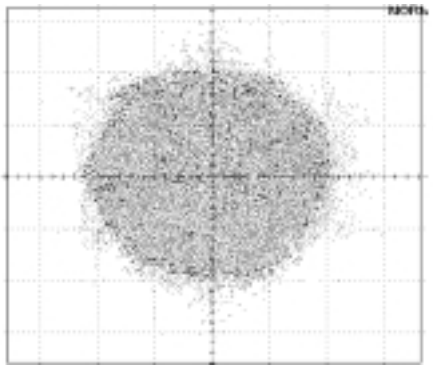

Fig. 16b: The current error space phasor boundary
[X axis, Y axis: 1 div = 0.3 Amp]

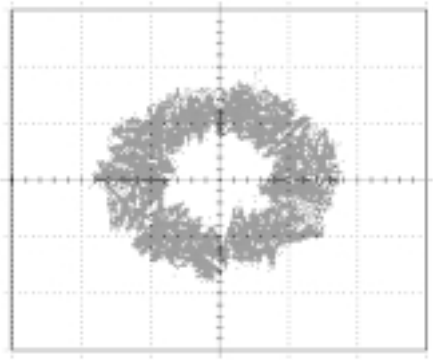

Fig.16c: The machine current space phasor (no –load)
[X-axis: Y-Axis: 1 div = 1 Amp]

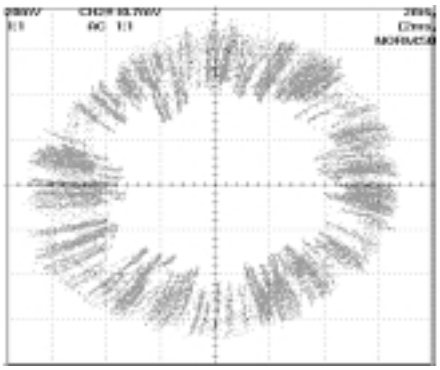

Fig. 16d: The machine current space phasor when loaded
[X-axis:Y-Axis: 1 div = 1 Amp]

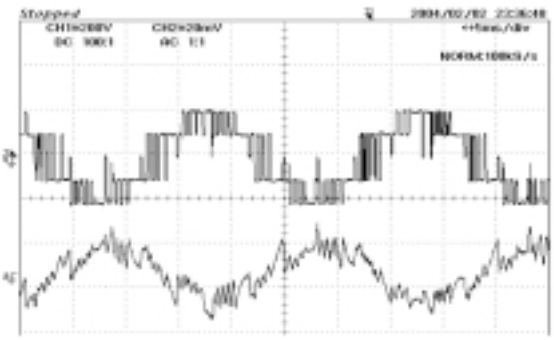

Fig.16e: The machine phase voltage and current during over modulation [x axis: 1 div = 200 V y-axis: 1 div = 2 Amp]

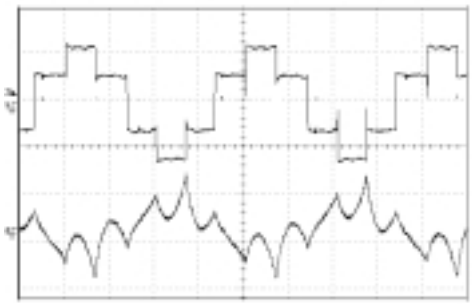

Fig. 16f: The machine phase voltage and current during six step mode [x axis: 1div = 200 V y-axis: 1 div = 2 Amp]

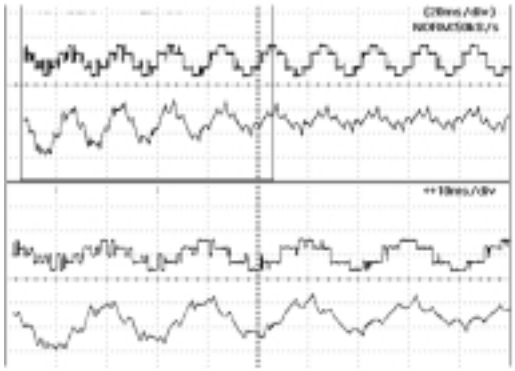

Fig. 16g: The phase voltage and phase current during transition to six step [Y axis: 1 div = 400 V (top trace) 1 div = 4 Amp] The bottom traces are the zoomed view of the window shown in the top traces, which show the transition to six step

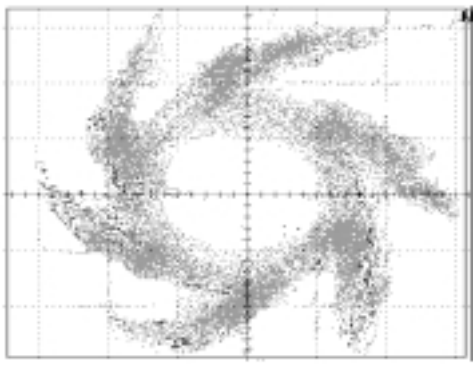

Fig. 16h: The error space phasor boundary during six step operation DAC output [X-axis, Y-Axis: 1 div = 1 amp]

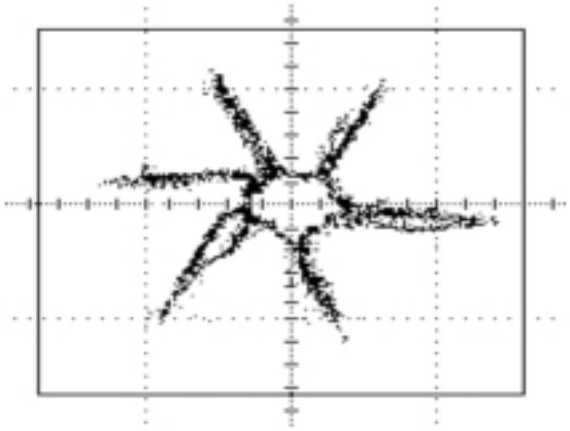

Fig. 16i: The machine current space phasor during over modulation [X-axis, Y-axis 1 div = 3 amp]

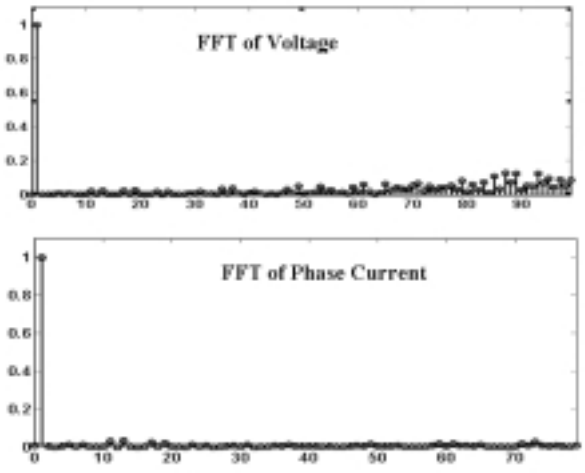

Fig. 16j: The normalised harmonic spectrum phase voltage (top) and Phase current (Corresponding to Fig. 16a)

Fig.16a shows the phase voltage current when the motor is running in the linear range and the phase voltage profile indicates that adjacent vectors are always selected. The phase current is controlled within the band and is smooth during the sector change. Fig.16b shows the error space phasor boundary. The error is kept within the boundary all times except during the sector changes where it briefly crosses the error boundary. Fig.16c shows the machine current space phasor, which shows the rotating space phasor whose amplitude is kept within the hysteresis band. Fig.16d shows the current space phasor, when the motor is loaded, and it shows a circular profile for the actual machine current space phasor.

Fig.16e shows the machine voltage and current for high speed, where the drive is running in the over modulation region. The profile of machine voltage and current show the typical over modulation characteristics. Fig. 16f shows the motor voltage current during the six-step operation and in Fig. 16g the transition to the six step operation is captured as the motor is accelerated to the full speed. Fig.16h shows the current error space phasor boundary during the six step operation and in Fig. 16i, the current space phasor during six step operation is shown. The nature of the current error space boundary and the current space phasor during six step show similar shapes as obtained in simulation results (Fig. 14.d). The normalised harmonic spectrum of the machine phase voltage and phase current (Fig. 16a) are shown in Fig. 16j. The spectrum shows the absence of the sub-harmonic components and reduced low order harmonics.

Conclusion

A self-adapting space phasor based current hysteresis controller is proposed in this paper for three phase voltage source PWM inverters. The current errors are controlled along three axes j_A, j_B, j_C which are perpendicular to the A, B, C phases respectively and the current error space phasor is held within a hexagonal boundary. The proposed controller achieves optimum PWM switching by ensuring that always inverter voltage vectors adjacent to the machine voltage vector are selected and also ensures that only one inverter leg is switched during an inverter switching transition. It does not use any computation of the machine voltage and the inverter voltage vectors are selected using a simple look-up table. The proposed controller uses a self adaptive region detection logic which ensures selection of a the unique inverter vector (among the adjacent vectors) for all regions of the boundary. The proposed method uses a simple self adapting logic for sector changes and achieves smooth transition to the six step operation, with simple look-up tables. The controller is implemented for a 5hp induction motor drive and the experimental results are presented.

Reference

[1] M. P. Kazmierkoswki, and Luigi Malesani: Current control techniques for three phase voltage source PWM converters:A survey, IEEE Trans.Ind.Electronics, Vol. 45, No. 5, Oct 1998, pp 691-703.

[2] M. P. Kazmierkowski and W. Sulkowski: A novel vector control scheme for transistor inverter fed induction motor drive, IEEE Trans. Ind. Electron., vol. 38, no.1, pp.41-47, Feb. 1991

[3] D. M. Brod, D. W. Novotny: Current control of VSI-PWM inverters, IEEE Trans. Ind. Appl. Vol.1A-21, No.4, May/June 1985., pp 562-570

[4] J. Holtz: Pulsewidth Modulation- A survey, IEEE Trans. Ind. Electronics, Vol. 39, No.5, December 1992, pp 410-420

[5] S. Salama and S. Lennon: Overshoot and limit cycle free current control method for PWM Inverters, in Proc. EPE European. Conf. Power Electron. Appln., Florence, Italy, 1991,pp 3/217- 222.

[6] A. Kawamura and R.G Hoft: Instantaneous feedback controlled PWM inverters with adaptive hysteresis; IEEE Trans. Ind. Appln., vol.IA-20, pp.769-775, July/Aug.1984.

[7] L. Malesani, L. Rossetto, L. Sonaglioni, P. Tomasin and A. Zuccato: Digital adaptive hysteresis current control with clocked communications and wide operating range, IEEE Trans. Ind. Appln., vol.IA-32, pp.1115-1121, March/April 1996

[8] L. Malesani, and P. Tenti: A novel hysteresis control method for current controlled VSI PWM inverters with constant modulation frequency; IEEE Trans. Ind. Appln., vol.IA-26, pp.88-92, Jan/Feb.1990.

[9] W. McMurray: Modulation of the Chopping Frequency in DC Choppers and PWM Inverters Having Current-Hysteresis controllers; Conf.Proceedings PESC'83, pp. 295-299.

[10] G. Pfaff, A. Weschta and A. Wick: Design and experimental results of a brush less AC servo drive, IEEE IAS conf., 1982, pp 692-697.

[11] J. Holtz, S.Stadtfield: A PWM inverter drive system with on-line optimised pulse pattern, in EPE European Conf. Power Electron.Appl., Brussels, Belgium, 1985, pp.779-788.

[12] A. Nabae, S. Ogosawara and H. Akagi: A novel control scheme for current controlled PWM inverters, IEEE Trans.Ind.Appl., Vol.1A-22,No.4,July/Aug 1986, pp 697-701.

[13] M. P. Kazmierkoswki, M. A. Dzieniakowski and W. Sulkowski: Novel space phasor based current controllers for PWM-Inverters, IEEE Trans. Power Electronics, Vol.6, No.1, Jan. 1991, pp 158-166.

[14] I. Nagy, Z. Suto, L. Latakas Jr., E. Masada: Features of adaptive PWM explored by the theory of chaos", in 6th European Conference on Power Electronics and Applications, EPE'95, Sevilla, Spain, Sept. 1995, Vol.3, pp 1013-1018.

[15] I. Nagy: Control Algorithm of a three phase voltage sourced reversible rectifier; Proc. EPE European. Conf. Power Electron. Appln., Florence, Italy, 1991, pp 3/287-292.

[16] B. H. Kwon, T. W. Kim and J. H. Youm: Novel SVM based hysteresis current controller", IEEE Trans. Power. Electronics, Vol.13, No.2, March 1998., pp 297-307.

[17] Vinay Mistry, S. P. Waikar, K. Gopakumar, L. Umanand, V. T. Ranganathan: A multi axis space phasor based current hysteresis controller for PWM Inverters",EPE Journal, Vol.10. No.1, April 2000, pp 17-25.

The Authors

M. R. Baiju received his B.Tech degree in Electronics and Communication Engineering from College of Engineering, Trivandrum in 1988 and M.Tech. and Ph.D from CEDT, Indian Institute of Science in 1997 and 2004, respectively. From 1988 to 1991 he was with the National Thermal Power Corporation Ltd., New Delhi and since 1991 he has been a faculty at College of Engineering, Trivandrum.

Krishna K. Mohapatra received the B.E. degree from R.E.C. Rourkela, India and M.Tech degree from Indian Institute of Technology, Kharagpur in 1993 and 1996, both in Electrical Engineering. He was a design and development engineer in National Radio and Electronics Company Ltd., from 1995 to 2000. He obtained his Ph.D degree in 2003, from the Centre for Electronics design and Technology, Indian Institute of Science, Bangalore, India. His research interests are in the area of Power converters, PWM strategies and Motor Drives. He is currently pursuing postdoctoral fellowship at University of Minnesota, USA.

R. S. Kanchan received the B.E. degree in electrical engineering from the Walchand College of Engineering, Sangli, India, in 1998, the M. Tech. degree in electrical engineering from the Indian Institute of Technology, Bombay, India in 2000, and is currently pursuing the Ph. D. degree at the Centre for Electronic Design and Technology (CEDT), Indian Institute of Science, Bangalore, India. He was with Tata Steel Company from 2000 to 2002.

P. N. Tekwani received his B.E. degree in power electronics from the Lakhdhirji Engineering College, Morbi, India, in 1995, the M.E. degree in electrical engineering from the Maharaja Sayajirao University, Vadodara, India, in 2000, and is currently pursuing the Ph. D. degree at the Centre for Electronic Design and Technology (CEDT), Indian Institute of Science, Bangalore, India. From 1996 to 2001, he was with Electrical Research and Development Association (ERDA), Vadodara, India, and since 2001 he has been a Member of the Faculty at the Nirma Institute of Technology, Ahmedabad, India.

K. Gopakumar received his B.E., M.Sc.(Engg.) and Ph.D. degrees from Indian Institute of Science in 1980,1984 and 1994 respectively. He was with the Indian Space Research organization from 1984 to 1987. He is currently Associate Professor at CEDT(centre for Electronics Design and Technology), Indian Institute of Science, Bangalore-560012, India. His fields of interest are Power Converters, PWM Techniques and AC Drives.